Published in final edited form as:
Nature. 2020 January ; 577(7788): 127–132. doi:10.1038/s41586-019-1808-9.

α-Synuclein regulation by chaperones in mammalian cells

Björn M. Burmann[#1,2,3,*], **Juan A. Gerez**[#4], **Irena Matečko-Burmann**[1,3,5], **Silvia Campioni**[4,7], **Pratibha Kumari**[4], **Dhiman Ghosh**[4], **Adam Mazur**[1], **Emelie E. Aspholm**[2,3], **Darius Šulskis**[2,3], **Magdalena Wawrzyniuk**[6], **Thomas Bock**[1], **Alexander Schmidt**[1], **Stefan G.D. Rüdiger**[6], **Roland Riek**[4,*], **Sebastian Hiller**[1,*]

[1]Biozentrum, University of Basel, Klingelbergstr. 70, 4056 Basel, Switzerland [2]Department of Chemistry and Molecular Biology, University of Gothenburg, 405 30 Göteborg, Sweden [3]Wallenberg Centre for Molecular and Translational Medicine, University of Gothenburg, 405 30 Göteborg, Sweden [4]Laboratory of Physical Chemistry, Department of Chemistry and Applied Biosciences, Eidgenössische Technische Hochschule Zürich, Wolfgang-Pauli-Str. 10, 8093 Zurich, Switzerland [5]Department of Psychiatry and Neurochemistry, University of Gothenburg, 405 30 Göteborg, Sweden [6]Cellular Protein Chemistry, Bijvoet Center for Biomolecular Research, Utrecht University, Padualaan 8, 3584 CH Utrecht, The Netherlands

[#] These authors contributed equally to this work.

Abstract

Neurodegeneration in Parkinson's disease is correlated with the occurrence of Lewy bodies, intracellular inclusions containing aggregates of the intrinsically disordered protein (IDP) α-Synuclein[1]. The aggregation propensity of α-Synuclein in cells is modulated by specific factors including posttranslational modifications[2,3], Abelson-kinase-mediated phosphorylation[4,5] and interactions with intracellular machineries such as molecular chaperones, although the underlying mechanisms are unclear[6–8]. Here, we systematically characterize the interaction of molecular chaperones with α-Synuclein *in vitro* as well as in cells at the atomic level. We find that six vastly different molecular chaperones commonly recognize a canonical motif in α-Synuclein, consisting

[*]Correspondence and requests for materials should be addressed to BMB, RR, and SH. bjorn.marcus.burmann@gu.se, roland.riek@phys.chem.ethz.ch, sebastian.hiller@unibas.ch.
[7]Present address: Cellulose & Wood Materials Laboratory, Department of Functional Materials, Empa, Überlandstrasse 129, 8600 Dübendorf, Switzerland

Author contributions

B.M.B. expressed, purified chaperones, and performed NMR experiments. B.M.B. and S.C. expressed and purified α-Synuclein variants with help of P.K.. E.E.A. and D.Š. supported protein purification of chaperones as well as α-Synuclein variants. J.A.G. prepared and performed in-cell NMR experiments as well as chaperone knock-down experiments and immunofluorescence experiments. S.C. and D.G. performed the aggregation assays. I.M.-B. performed cell culture experiments, prepared lipid vesicles, performed and analyzed MS-experiments together with T.B. and A.S.. A.M. performed model calculations. M.W. and S.G.D.R. provided purified Hsp90β for interaction studies. B.M.B., S.C., R.R., and S.H. designed the study, analyzed the data, and wrote the manuscript with input from all co-authors.

The authors declare no competing financial interests.

Data availability statement

The data that support the findings of this study are available from the corresponding authors upon request.

Europe PMC Funders Author Manuscripts

of the amino-terminus and a segment around Tyr39, hindering its aggregation. In-cell NMR experiments[9] show the same transient interaction pattern preserved inside living mammalian cells. Specific inhibition of the interactions between α-Synuclein and the chaperones Hsc70 and Hsp90 yields transient membrane binding and triggers a remarkable re-localization of α-Synuclein to mitochondria and concomitant aggregate formation. Phosphorylation of α-Synuclein at Tyr39 directly impairs the chaperone interaction, thus providing a functional explanation for the role of Abelson kinase in Parkinson's disease progression. Our results establish a master regulatory mechanism of α-Synuclein function and aggregation in mammalian cells, extending the functional repertoire of molecular chaperones and opening new perspectives for therapeutic interventions for Parkinson's disease.

α-Synuclein–chaperone interaction at atomic detail

Based on previous findings that molecular chaperones share common patterns of client recognition[10,11], we characterized the interactions of an array of molecular chaperones with α-Synuclein. The array included human Hsc70 and Hsp90β, and bacterial chaperones SecB, Skp, SurA, and Trigger Factor, featuring strongly diverse architectures[10]. Any of these chaperones interferes functionally with α-Synuclein aggregation in a Thioflavin T (ThT) assay[6,8,12], already at 1:20 sub-stoichiometry, and with stronger effects at 1:10 ratios (Figs. 1a–c). The known Hsp90β inhibitors Geldanamycin and Radicicol (referred to onwards as drugs) decreased the chaperoning effect of Hsp90β (Fig. 1c), in line with the known mechanism of these drugs[13,14]. We determined the segments of α-Synuclein interacting with the individual chaperones at the atomic level by measuring NMR signal intensity attenuations and chemical shift perturbations in 2D [^{15}N,^{1}H]-NMR spectroscopy. For all six chaperones, the effects were most pronounced for twelve amino acid residues at the N-terminus and for six residues around Tyr39, indicating a direct albeit transient intermolecular interaction *via* these two segments, which are thus identified as the canonical chaperone-interaction motif of α-Synuclein (Fig. 1d–g; Extended Data Figs. 1,2). Inhibiting Hsp90β by drugs affected the interaction with α-Synuclein partially and for Hsc70 the interaction was observed in the ADP– and the ATP–bound, but not in the apo–state (Fig. 1g; Extended Data Fig. 3), in line with earlier reports[6,15,6,16] (see Supplemental discussion). Importantly, for all six chaperones, the interaction is observed at protein concentrations of 100 μM, far away from possible non-specific effects of macromolecular crowding. We probed such non-specific effects with high concentrations of either bovine serum albumin (BSA) or ubiquitin. No signal attenuations were observed for 150–310 mg/ml ubiquitin, ruling out macromolecular crowding effects. For high concentrations of BSA the canonical chaperone interaction signature is observed (Fig. 1g; Extended Data Figs. 3d–j), due to BSA's weak molecular chaperone function[17]. Together, the experiments on an array of six chaperones and two control proteins revealed a canonical chaperone interaction for α-Synuclein at the amino-terminus and around Tyr39, transient in nature. Notably, it comprises the two locally most hydrophobic segments of α-Synuclein (Extended Data Fig. 3k,l), indicating an importance of hydrophobic residues for the chaperone interaction.

Towards characterizing the physiological role of chaperone–α-Synuclein interactions, we determined the affinity of α-Synuclein to Hsc70$_{ADP}$, SecB, and Skp by Bio-Layer

Interferometry (BLI). α-Synuclein binds each of these chaperones with affinities ranging 1–2 μM (Extended Data Fig. 4 and Supplementary Table S1). The variant ΔN–α-Synuclein lacking 10 amino-terminal residues, has an affinity decreased by two orders of magnitude, validating this segment as part of the interaction site. At the reported cellular concentrations of α-Synuclein in neuronal synapses of ~50 μM with a combined concentration of Hsp70/Hsp90 chaperones of ~70μM[18], about 90% of cellular α-Synuclein can thus be chaperone-bound.

We then analyzed published data on the NMR intensity profile of α-Synuclein inside living mammalian cells, which strikingly feature the canonical chaperone interaction signature[9]. Because this pattern was suggested to arise from interactions with cellular membranes, we probed the interaction of α-Synuclein with soluble cellular extracts. α-Synuclein in either 25 mg/ml *E. coli* cell-extract or 50 mg/ml soluble extracts from two mammalian cell lines, HEK-293 or MDCK-II, showed the canonical chaperone interaction pattern (Fig. 1h; Extended Data Figs. 5a–d), thus experimentally reproducing the in-cell interaction pattern in the absence of membranes[9]. Furthermore, we characterized the interaction pattern of α-Synuclein with lipid bilayer membranes *in vitro*[19]. Titrating LUVs (Large unilamellar vesicles) to α-Synuclein in a 125:1 lipid:protein ratio lead to a uniform NMR signal decrease for residues 1–90 (Extended Data Fig. 6a), in full agreement with published reports[9,19]. Adding 2–6 equivalents of SecB to α-Synuclein–LUV solutions restored the chaperone signature, whereas the reverse experiment, addition of LUVs to an existing SecB–α-Synuclein complex led to global signal attenuation for residues 1–90 with substantially reduced effect, indicating that LUVs and SecB mutually compete for α-Synuclein binding (Extended Data Fig. 6). Overall, α-Synuclein thus populates an equilibrium between its free state, its membrane-bound state, and its chaperone-bound state, with the latter two being mutually exclusive. The emerging hypothesis that in mammalian cells α-Synuclein is dominantly in contact with chaperones rather than with lipid bilayers was supported by an experimental determination of the interactome of the α-Synuclein amino-terminus in mammalian cells by chemical cross-linking and mass-spectrometry. The interactome consists of a large number of molecular chaperones in the range of 30–75% abundance, including several Hsp90-variants and six Hsp70-variants (Fig. 2a; see Supplemental for details).

In-cell NMR spectroscopy

Next, we carried out in-cell NMR experiments to study the interaction of α-Synuclein with chaperones inside living mammalian cells at atomic resolution. [*U*-^{15}N]–α-Synuclein was delivered into HEK-293 cells at a concentration of 3–10 μM, yielding intensity patterns characteristic for mammalian cell-lines[9] (Figs. 2b–c), comprising the canonical chaperone–interaction signature and its transient nature. Multiple molecular chaperones are present in the cell, with mutually overlapping functions and "clientomes"[20]. In line with our *in vitro* chaperone array, we probed the two constitutively most expressed eukaryotic chaperones Hsc70 and Hsp90β. When [*U*-^{15}N]–α-Synuclein was delivered into cells with reduced Hsc70 levels (Extended Data Figs. 7c,d), the NMR intensity profile resembled the one observed for normal cells, suggesting a functional redundancy with other cellular chaperones (Figs. 2d,e). Next, we treated cells with the Hsp90-inhibiting drugs, and found that the

canonical chaperone interaction motif showed increased intensities compared to untreated cells (Fig. 2d). This suggests that Hsp90 chaperones physically interact with α-Synuclein in normal cells transiently, and that this interaction is lost upon drug treatment. Immunoprecipitation assays confirmed an almost complete loss of this interaction at 24 hours post-treatment (Extended Data Fig. 7e). Finally, we inhibited both Hsc70 and Hsp90β chaperones simultaneously, observing a moderate effect on the canonical interaction motif already at 4 hours post-treatment, when a significant fraction of Hsp90 still remains bound to α-Synuclein (Extended Data Fig. 7e). At this time point, a low but measurable amount of free intracellular α-Synuclein was observed (Fig. 2d). At 24 hours post-treatment, a dramatic global signal reduction for residues 1–90 was observed, essentially identical to the LUV interaction pattern, as well as to the profile reported for α-Synuclein binding bacterial membranes[19,21] (Figs. 2d,f). The combined inhibition of the two chaperones types Hsc70 and Hsp90 thus leads to a transient membrane interaction of α-Synuclein, absent in the cellular ground state. In parallel, upon suppressing both chaperones we observed the formation of macroscopic aggregates containing α-Synuclein (Extended Data Figs. 7f). Overall, these in-cell NMR and *in vitro* experiments show that in normal cells α-Synuclein is physically and transiently interacting with a pool of constitutively expressed chaperones and that this interaction dominates over α-Synuclein's transient interaction with membranes. In typical cells including neurons[18,22], as well as in our in-cell experiments the concentration of chaperones is substantially larger than the concentrations of α-Synuclein, underlining the physiological relevance of these observations (Extended Data Figs. 7g,h).

Intracellular membrane localization

The interaction of α-Synuclein with cellular membranes upon Hsc70/Hsp90 inhibition may be a key mechanism for disease pathogenesis and we thus aimed at identifying the involved membranous organelle by co-localization. To this end, control cells and HEK-293 cells depleted of Hsc70 and treated with drugs for 24 hours, stained with mitotracker (stains mitochondria), lysotracker (stains acidic vesicles, e.g. lysosomes), or Alexa-Fluor-labeled wheat germ agglutinin (WGA, stains plasma membrane and endoplasmic reticulum), and subsequently immunostained with anti-α-Synuclein antibodies. These experiments revealed a strong co-localization of α-Synuclein with mitochondria upon depletion of chaperones (Fig. 3a–c). To further confirm this association, we carried out immunofluorescence analyses using antibodies specific for the mitochondrial marker CoxIV and α-Synuclein (Fig. 3d), as well as the mitochondrial marker mtBFP (mitochondrial blue fluorescent protein) in control and in HEK-293 cells with impaired Hsc70 and Hsp90 activity (Figs. 3e,f). Both additional approaches confirmed the localization of α-Synuclein to mitochondria upon chaperone inhibition.

Effect of posttranslational modifications

Having established the canonical chaperone interaction signature, and validated its presence in living cells, we investigated the effect of chemical modifications on the α-Synuclein–chaperone interaction. Using the chaperones Hsp90β, $Hsc70_{ADP}$, SecB, and Skp, we probed the effects of amino-terminal acetylation of α-Synuclein, the predominant form in mammalian cells[9,19]. Acetylation does not interfere with the chaperone interaction (Fig. 4;

Extended Data Figs. 8a–g). In contrast, ΔN–α-Synuclein features a completely reduced interaction with all chaperones, in full agreement with the BLI experiments, and revealing a synergistic effect between the amino-terminus and the stretch around Tyr39 (Figs. 4b–e). Cellular oxidative stress and reactive oxygen species imbalance are known hallmarks of Parkinson's disease onset, leading to oxidative modification of α-Synuclein[2]. Titrating of Hsp90β, $Hsc70_{ADP}$, SecB or Skp to methionine-oxidized α-Synuclein[23] showed that oxidation of Met1 and Met5 abolish the amino-terminal interaction (Fig. 4, Extended Data Fig. 9). To explore the effects of phosphorylation on chaperone interaction, we employed *in vitro* tyrosine-phosphorylation with different kinases[5,24] (Fig. 4; Extended Data Fig. 9). Titration of SecB, Skp, Hsp90β, or $Hsc70_{ADP}$ to either tetra-phosphorylated or Tyr39-mono-phosphorylated α-Synuclein resulted in elimination of the chaperone interaction, whereas Tyr125-Tyr133-Tyr136-tri-phosphorylated α-Synuclein showed the chaperone interaction pattern of unmodified α-Synuclein (Fig. 4). Tyr39 phosphorylation thus has a specific inhibitory effect towards chaperone interaction, providing a direct rationale for *in vivo* studies showing that up-regulation of c-Abl correlates strongly with Tyr39-phosphorylation and disease progression in Parkinson's disease[5,25].

Conclusion

Overall, in this work we have identified a functional mechanism for regulation of α-Synuclein by chaperones in mammalian cells through transient binding (Extended Data Fig. 10). Molecular chaperones bind the IDP α-Synuclein *via* a canonical motif, based on recognizing intrinsic biophysical features. The interaction vanishes upon inhibition of two main chaperones, resulting in transient membrane interactions and an accumulation of α-Synuclein at mitochondria, a major component of Lewy bodies[26,27]. A functional model emerges, where transient chaperone-interacting forms are the dominant species of α-Synuclein in healthy cells, making chaperones a master regulator of the cellular states of α-Synuclein. It predicts that changes in the cellular levels of either chaperones or α-Synuclein, or the modulation of their interaction will disturb the homeostatic balance, eventually causing Parkinson's disease. Notably, this model agrees with a plethora of reported experimental observations (see Supplemental for an extended discussion), including that the ratio of α-Synuclein to chaperone is impaired by familial Parkinsonism and that oxidative stress can lead to an increase of α-Synuclein Tyr39-phosphorylation[5,25], which interferes with chaperone binding. The model shows further how modulation of chaperone activity might prevent the formation of oligomeric α-Synuclein, leading to mitochondrial membrane disruption[28] and also accounts for recent reports that impairment of mitochondria may constitute an important factor in Parkinson's disease[29–31].

Extended Data

Europe PMC Funders Author Manuscripts

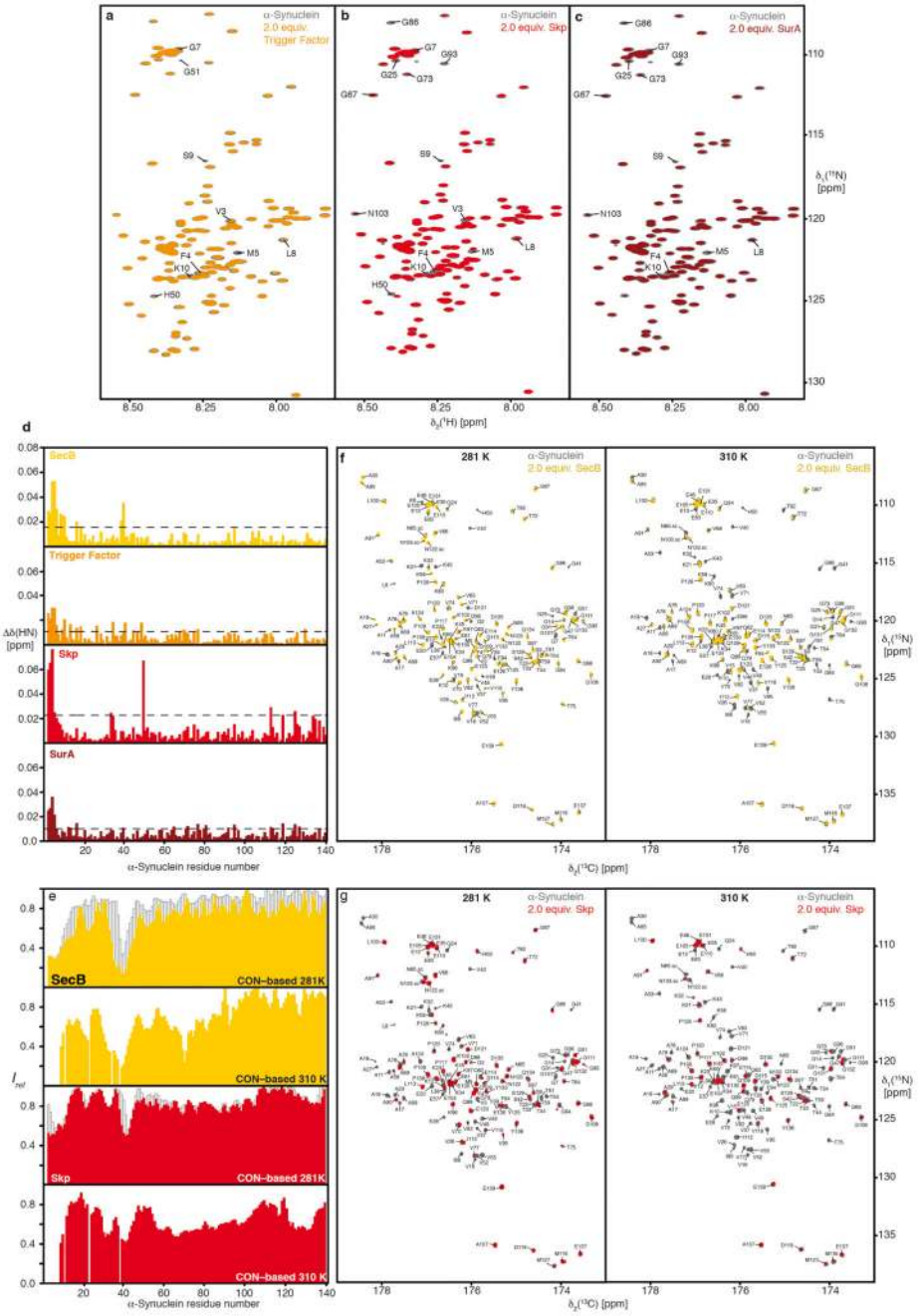

Extended Data Figure 1. Interaction between α-Synuclein and bacterial chaperones.

a–c, Overlay of 2D [^{15}N,^{1}H]-NMR spectra of 250 μM [*U*-^{15}N]–α-Synuclein in the absence (grey) and presence of 500 μM chaperones, as indicated. The sequence-specific assignments for significantly affected resonances are indicated. **d,** Residue-resolved chemical shift perturbations of α-Synuclein caused by the addition of two equivalents of either SecB-tetramer (yellow), Trigger Factor dimer (orange), Skp trimer (red), and SurA dimer (dark red). Broken lines indicate a significance level of two standard deviations of the mean. **e,** Temperature-dependence of the α-Synuclein interaction with either SecB (yellow) or Skp

(red) monitored by residue-resolved intensity ratios ($I_{rel} = I/I_0$) of ^{13}C-direct detected 2D [^{15}N,^{13}C]–NMR spectra. The intensity ratios of 2D [^{15}N, ^{1}H]–NMR spectra at 281 K (Fig. 1**c**) are shown as an outline (grey). **f, g,** Overlay of 2D [^{13}C,^{15}N]-NMR spectra of 500 μM [*U*-^{13}C, ^{15}N]–α-Synuclein in the absence (grey) and presence of 1mM of SecB-tetramer ((**f**), yellow) or 1mM of Skp-trimer ((**g**), red). Experiments were performed at 281 K and 310 K as indicated. The sequence-specific resonance assignment is shown. Experiments in panels **a–c** and **f–g** were done in duplicates yielding similar results.

Europe PMC Funders Author Manuscripts

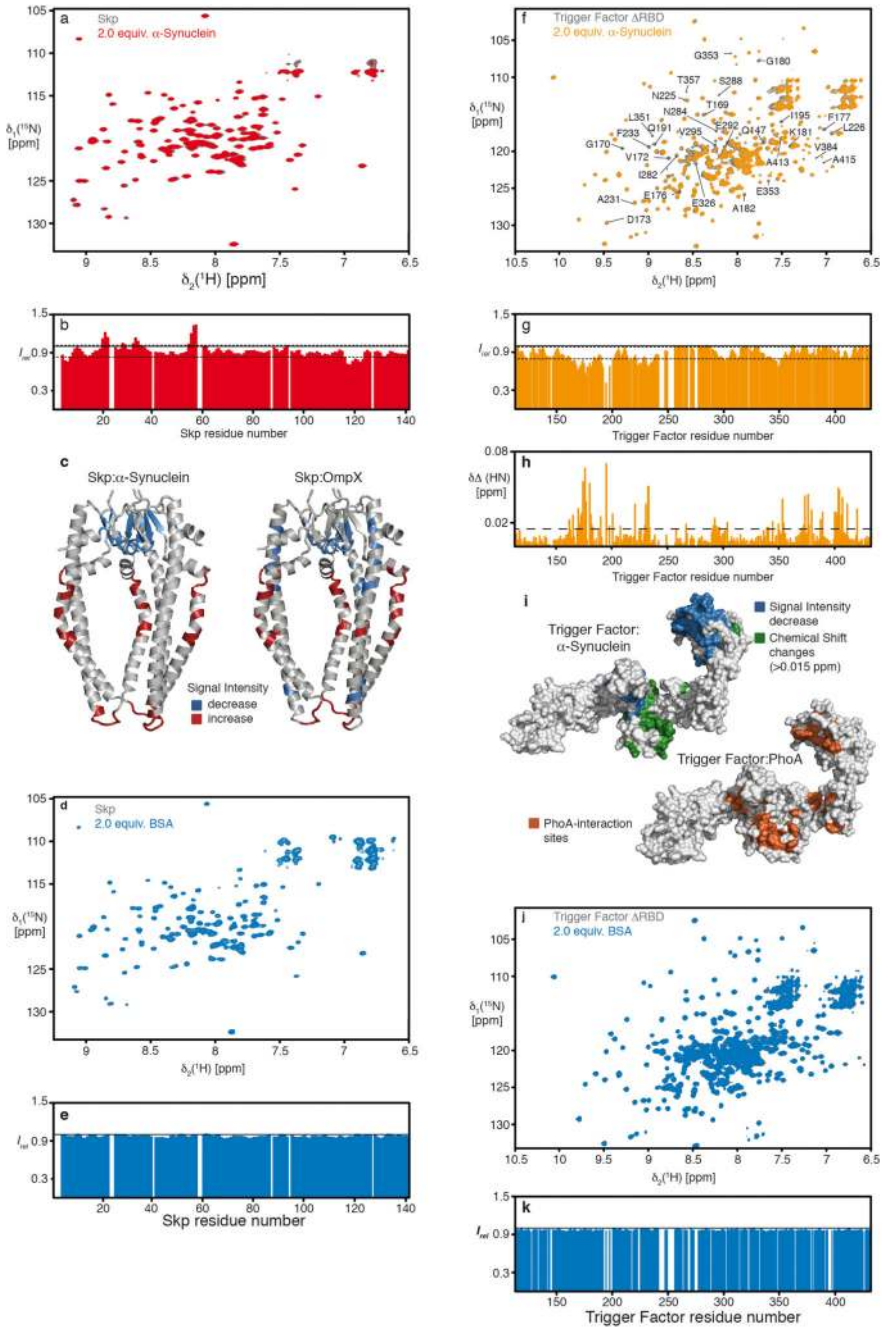

Extended Data Figure 2. Chaperones Skp and Trigger Factor bind α-Synuclein at their native client sites.

a, Overlay of 2D [^{15}N,^{1}H]-NMR spectra of 250 μM [*U*-^{2}H,^{15}N]–Skp in the absence (grey) and presence of 750 μM α-Synuclein (red). **b,** Residue-resolved NMR signal intensity ratios ($I_{rel} = I/I_0$) of Skp (250 μM) in the presence of three equivalents of α-Synuclein measured at 310K. The thin broken lines indicate a significance level of one standard deviation to the mean. The thick broken line represents an intensity ratio of 1. **c,** α-Synuclein induced intensity changes plotted on the Skp crystal structure (PDB 1SG2) [32] and earlier reported

Europe PMC Funders Author Manuscripts

effects upon binding of its native client OmpX [10]. Signal decrease of more than one standard deviation is highlighted in blue, whereas signal increase is highlighted in red. **d,** Overlay of 2D [^{15}N,^{1}H]-NMR spectra of 250 μM [*U*-^{2}H,^{15}N]–Skp in the absence (grey) and presence of 500 μM BSA (blue). **e,** Residue-resolved NMR signal intensity ratios ($I_{rel} = I/I_0$) of Skp (250 μM) in the presence of two equivalents of BSA measured at 310K. The thick broken line represents an intensity ratio of 1. **f,** Overlay of 2D [^{15}N,^{1}H]-NMR spectra of 250 μM [*U*-^{2}H,^{15}N]–TF(ΔRBD), a monomeric Trigger Factor variant lacking its ribosome binding and main dimerization domain, in the absence (grey) and presence of 750 μM α-Synuclein (orange). **g,** Residue-resolved NMR signal intensity ratios ($I_{rel} = I/I_0$) of 250 μM TF(ΔRBD) in the presence of three equivalents of α-Synuclein measured at 298K. The thin broken lines indicate a significance level of one standard deviation of the mean. The thick broken line represents an intensity quotient of 1. **h,** Residue-resolved combined chemical-shift differences of the amide moieties. The broken line indicates a significance level of two standard deviations of the mean. **i,** Significant chemical shift changes (green) and intensity decrease (blue) plotted on the Trigger Factor structure (PDB 1W26) [33]. Comparison to the published Trigger Factor interaction-sites of PhoA (orange) [34]. **j,** Overlay of 2D [^{15}N,^{1}H]-NMR spectra of 250 μM [*U*-^{2}H,^{15}N]–TF(ΔRBD) in the absence (grey) and presence of 500 μM BSA (blue). **k,** Residue-resolved NMR signal intensity ratios ($I_{rel} = I/I_0$) of TF(ΔRBD) (250 μM) in the presence of two equivalents of BSA measured at 298 K. The thick broken line represents an intensity ratio of 1. Experiments with α-Synuclein (panels **a** and **f**) were done as duplicates yielding similar results, whereas control experiments with BSA (panels **d** and **j**) were performed once.

Europe PMC Funders Author Manuscripts

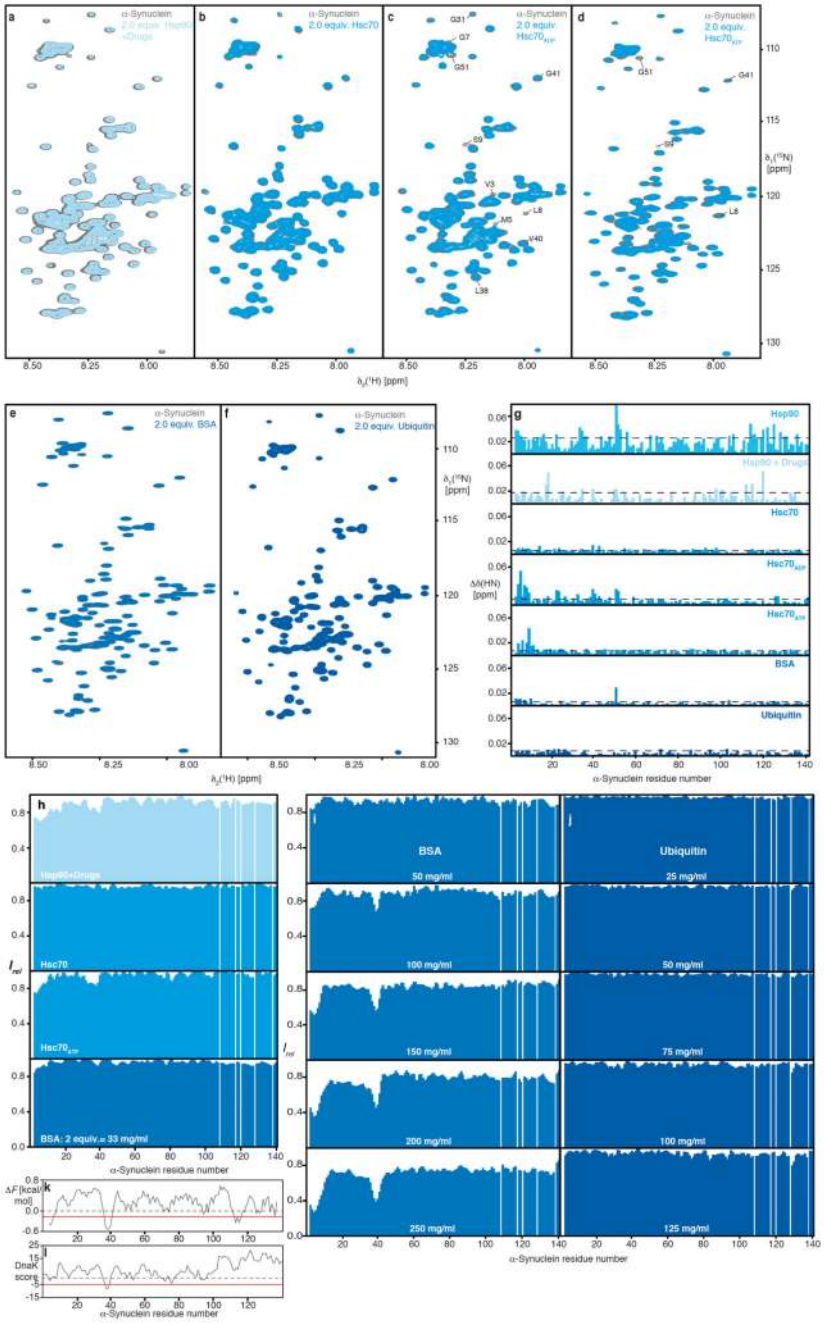

Extended Data Figure 3. Interaction between α-Synuclein and mammalian proteins.

a, Overlay of 2D [^{15}N,^{1}H]-NMR spectra of 25 μM [*U*-^{15}N]–α-Synuclein in the absence (grey) and presence of 50 μM inhibited Hsp90β-dimer (light blue). Measured in NMR-buffer plus 5 mM $MgCl_2$, 5 mM ATP, 1 μM Radicicol, and 1 μM Geldanamycin. **b,** Overlay of 2D [^{15}N,^{1}H]-NMR spectra of 100 μM [*U*-^{15}N]–α-Synuclein in the absence (grey) and presence of 200 μM Hsc70 (light blue). **c,** Overlay of 2D [^{15}N,^{1}H]-NMR spectra of 100 μM [*U*-^{15}N]–α-Synuclein in the absence (grey) and presence of 200 μM $Hsc70_{ADP}$ (light blue). Measured in NMR-buffer plus 5 mM $MgCl_2$ and 5 mM ADP. **d,** Overlay of 2D [^{15}N,^{1}H]-NMR spectra

Europe PMC Funders Author Manuscripts

of 100 μM [*U*-^{15}N]–α-Synuclein in the absence (grey) and presence of 200 μM $Hsc70_{ATP}$ (light blue). Measured in NMR-buffer plus 5 mM $MgCl_2$ and 5 mM ATP. **e,** Overlay of 2D [^{15}N,^{1}H]-NMR spectra of 250 μM [*U*-^{15}N]–α-Synuclein in the absence (grey) and presence of 500 μM (33 mg/ml) BSA (blue). **f,** Overlay of 2D [^{15}N,^{1}H]-NMR spectra of 250 μM [*U*-^{15}N]–α-Synuclein in the absence (grey) and presence of 500 μM of Ubiquitin (dark-blue). **g,** Residue-resolved combined chemical-shift perturbations of amide moieties upon addition of Hsp90β (cyan), inhibited Hsp90β (light cyan), Hsc70 (light-blue), $Hsc70_{ADP}$ (light-blue), $Hsc70_{ATP}$ (light-blue), BSA (blue), and Ubiquitin (dark blue). Broken lines indicate a significance level of two standard deviations of the mean. **h,** Residue-resolved backbone amide NMR signal attenuation ($I_{rel} = I/I_0$) of α-Synuclein caused by the addition of two equivalents of inhibited Hsp90β (light cyan), Hsc70 (light blue), $Hsc70_{ATP}$ (light blue), and BSA (blue). **i,** Residue-resolved NMR signal attenuation ($I_{rel} = I/I_0$) of 100 μM [*U*-^{15}N]–α-Synuclein upon addition of increasing BSA concentrations (50–250 mg/ml). **j,** Residue-resolved NMR signal attenuation ($I_{rel} = I/I_0$) of 50 μM [*U*-^{15}N]–α-Synuclein upon addition of increasing Ubiquitin concentrations (25–125 mg/ml). **k,** Local hydrophobicity of α-Synuclein plotted against the amino acid sequence. Δ*F* are the free energies of transfer of the individual amino acids from an aqueous solution to its surface [35]. Hydrophobicity corresponds to negative Δ*F* values. An exponentially weighted 7-window average was applied to the raw data, with the edges contributing 50%. The red line indicates the average value of 1.5 standard deviations of the mean, the chosen threshold for the identification of the most hydrophilic segments. **l,** Sequence-dependent DnaK score for α-Synuclein derived from a computational DnaK prediction algorithm [36]. Regions of the primary sequence with scores less than -5 (red line) are predicted to bind DnaK, a bacterial homolog of Hsc70. Experiments in panels **a–f** were done in duplicates with similar results.

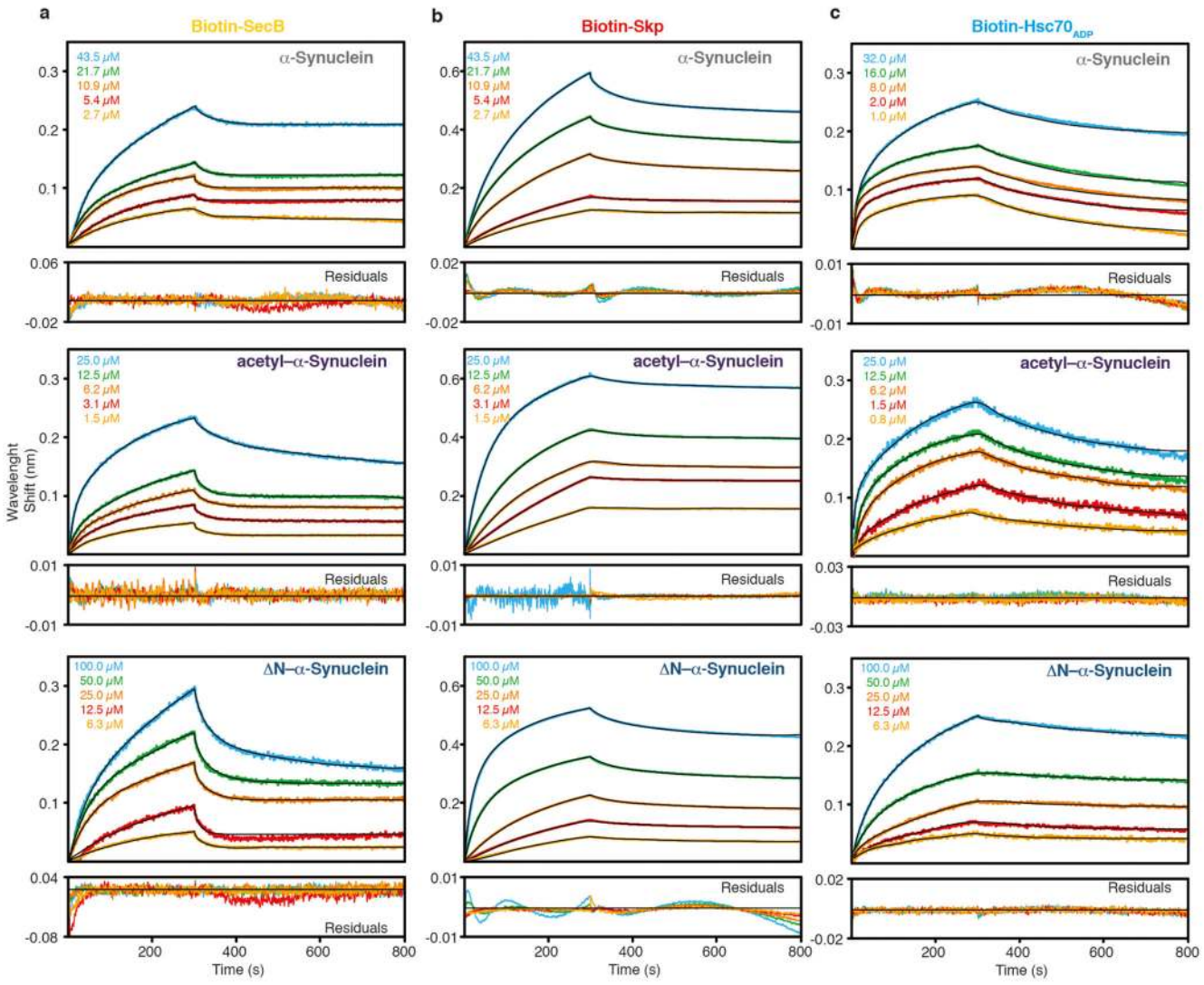

Extended Data Figure 4. Kinetic analysis of the interaction of the chaperones with α-Synuclein variants.

a–c, Kinetic analysis by BLI of biotinylated Skp (**a**), SecB (**b**), and $Hsc70_{ADP}$ (**c**) to different α-Synuclein-variants (α-Synuclein (top), acetyl–α-Synuclein (middle), and ΔN–α-Synuclein (bottom). Black lines represent least-square fits to the data. Below each set of BLI-curves the residuals of the fits are shown. Each individual kinetic experiment was run twice in triplicates with similar results.

Europe PMC Funders Author Manuscripts

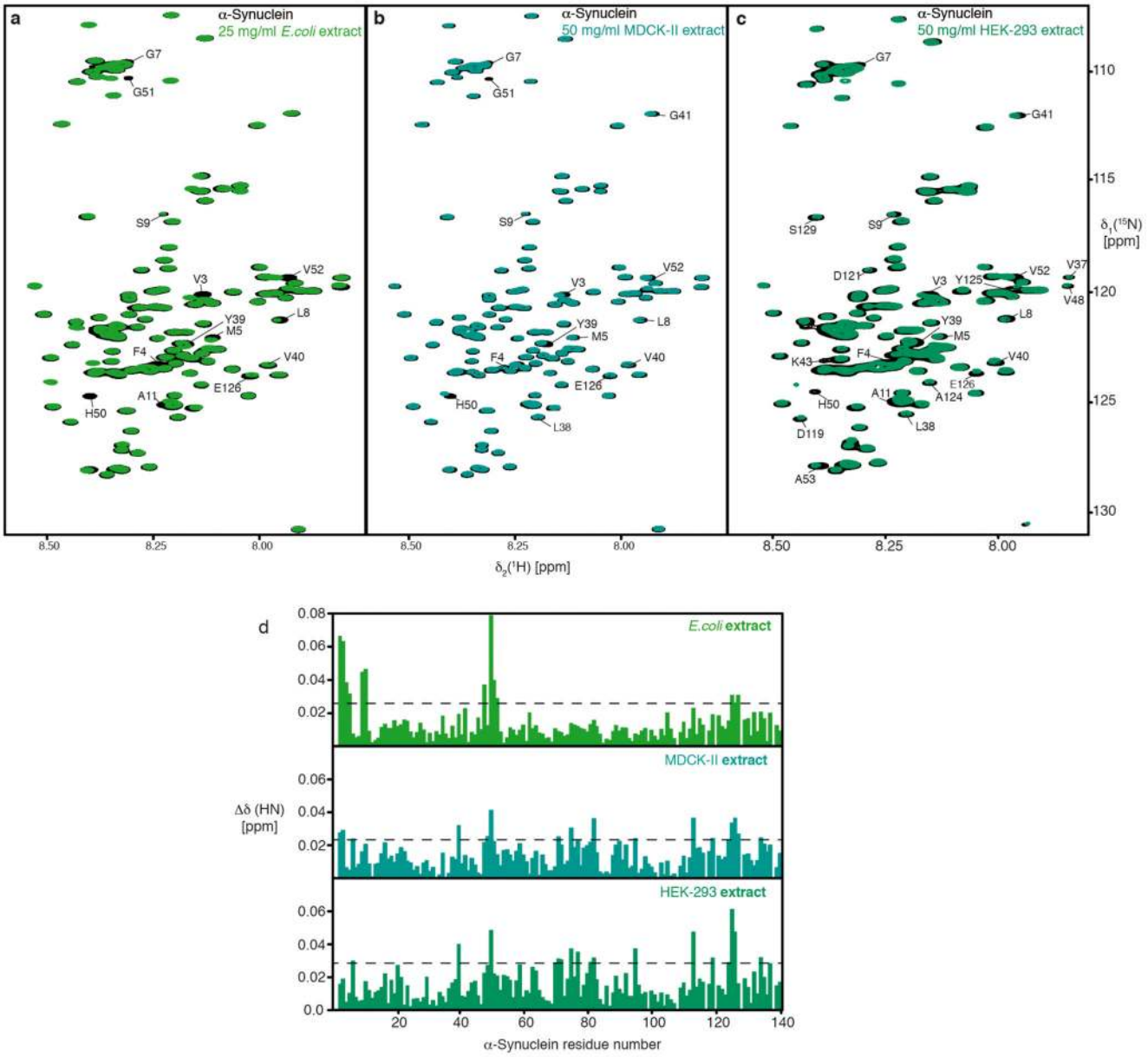

Extended Data Figure 5. Interaction between α-Synuclein and cellular extracts.

a, Overlay of 2D [^{15}N,^{1}H]-NMR spectra of 50 μM [*U*-^{15}N]–α-Synuclein in the absence (black) and presence of 25 mg/ml μM of *E. coli* cell extract (green). **b,** Overlay of 2D [^{15}N, ^{1}H]-NMR spectra of 50 μM [*U*-^{15}N]–α-Synuclein in the absence (black) and presence of 50 mg/ml mammalian MDCK-II cell extract (blue-green). **c,** Overlay of 2D [^{15}N,^{1}H]-NMR spectra of 50 μM [*U*-^{15}N]–α-Synuclein in the absence (black) and presence of 50 mg/ml mammalian HEK-293 cell extract (green). **d,** Residue-resolved combined chemical-shift perturbations of the α-Synuclein amide moieties in *E. coli* cell extract (green), mammalian MDCK-II cell extract (blue), and mammalian HEK-293 cell extract (green), all relative to aqueous buffer. Broken lines indicate a significance level of two standard deviations of the mean. Experiments in panels **a–c** were done in duplicates with similar results.

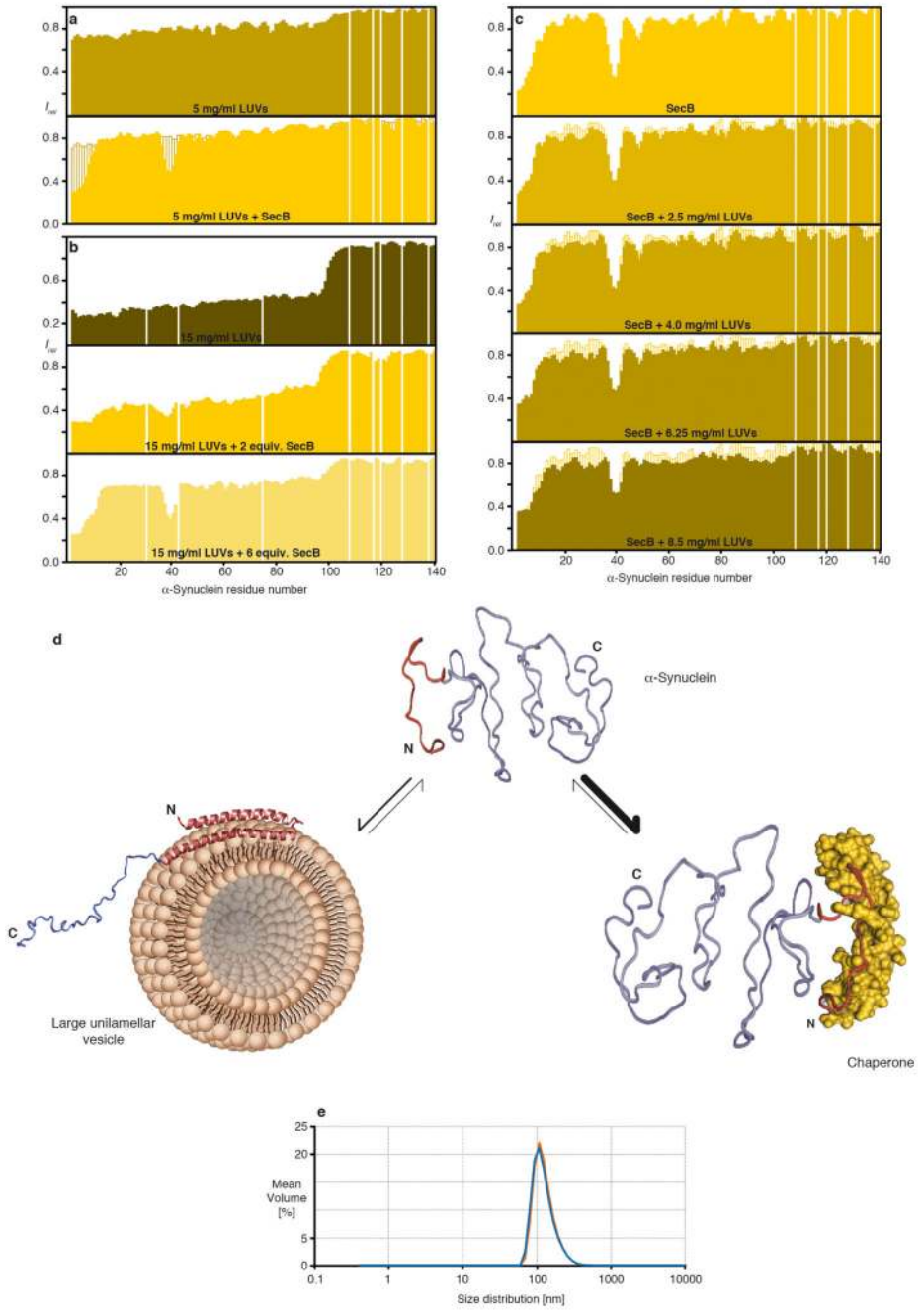

Extended Data Figure 6. LUVs and the chaperone SecB compete for α-Synuclein binding.

a, Residue-resolved backbone amide NMR signal attenuation ($I_{rel} = I/I_0$) of α-Synuclein caused by the addition of 5 mg/ml LUVs (125:1 molar ratio lipid:protein; dark yellow) and after further addition of two equivalents of SecB (yellow). **b,** Residue-resolved backbone amide NMR signal attenuation ($I_{rel} = I/I_0$) of α-Synuclein caused by the addition of 15 mg/ml LUVs (375:1 molar ratio lipid:protein; dark yellow) and after further addition of two and six equivalents of SecB, respectively (yellow), measured at 298 K. **c,** Residue-resolved backbone amide NMR signal attenuation ($I_{rel} = I/I_0$) of α-Synuclein caused by the addition

Europe PMC Funders Author Manuscripts

Europe PMC Funders Author Manuscripts

of 2 equivalents of SecB (yellow) and increasing amounts of LUVs with the following ratios: 2.5 mg/ml = 62.5:1, 4.0 mg/ml = 100:1, 6.25 mg/ml = 156:1, and 8.5 mg/ml = 212.5:1. **d,** Scheme showing the conformational equilibrium of free α-Synuclein, its chaperone-bound state, and one possible conformation of its LUV-bound state (PDB ID: 1XQ8) [19]. Notably, these observations are also in full agreement with related studies for Hsp90 [12] and Hsp27 [37]. **e,** Dynamic light scattering (DLS) measurements of LUVs prepared from pig brain polar lipids. Two independent preparations are shown in blue and orange, respectively, with an average diameter of 110 nm.

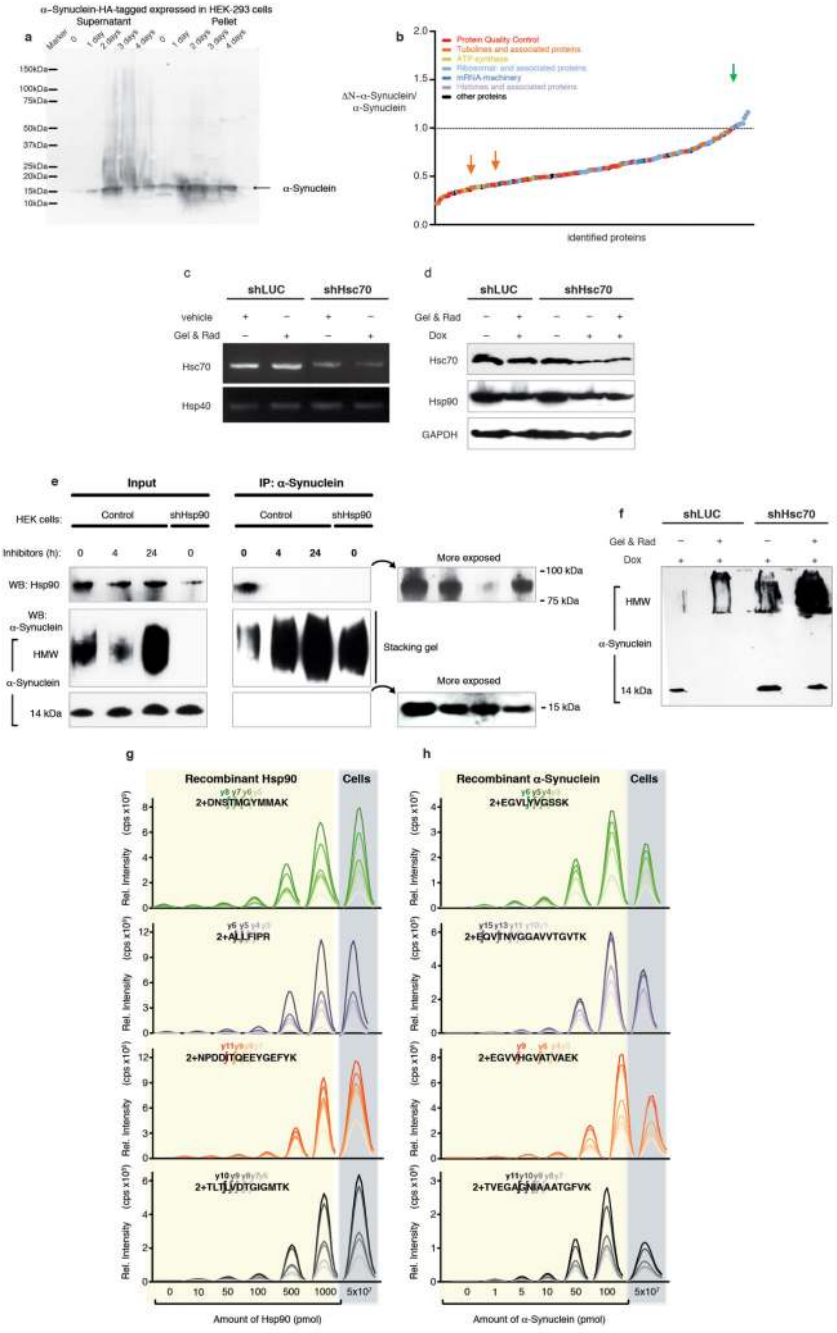

Extended Data Figure 7. In-cell interaction of α-Synuclein and chaperones.

a, Western blot analysis of expression of α-Synuclein fused to a carboxy-terminal HA-tag in HEK-293 cells. The molecular weight marker and the band corresponding to α-Synuclein-HA are indicated. With these samples immunoprecipitation and subsequent mass-spectrometric analysis was performed (Fig. 2a; Extended Data Fig. S7b). **b,** Intensity ratios of carboxy-terminally HA-tagged ΔN–α-Synuclein and α-Synuclein immune-precipitation determined by relative quantitative mass-spectrometry analysis. Experiments were performed as duplicates in HEK-293 cells. Identification of at least five peptides per protein

Europe PMC Funders Author Manuscripts

was required for quantification. Values: Mean. The dotted line represents an intensity ratio of 1. Proteins belonging to specific groups are highlighted in colors. Further, the values for α-Synuclein (green) as well as Tubulin β4 and Tubulin α1B (orange arrows from left to right) are indicated by colored arrows. **c,** Efficiency of Hsc70 knockdown in HEK-293 cells (constitutively expressing the T-Rex repressor) stably transfected with an inducible shRNA targeting Hsc70 mRNA (shHsc70). The image shows a representative semi-quantitative RT-PCR of Hsc70 mRNA in cells treated with doxycycline to induce shHsc70 and Geldanamycin (Gel) and Radicicol (Rad) for 24 hours (+). Cells transfected with a control shRNA targeting firefly luciferase (shLUC) as well as semi-quantification of an unrelated chaperone (Hsp40) were included as negative controls. **d,** Semi-quantification of Hsc70 and Hsp90 protein levels by Western blot. HEK-293 cells (constitutively expressing the T-Rex repressor) stably transfected with shHsc70 and shLUC were grown in normal (-) or doxycycline containing (+) medium for Hsc70 knockdown. The cells were subsequently treated with vehicle (-) or Geldanamycin and Radicicol (Gel & Rad) for Hsp90 inhibition. The constitutively expressed protein GAPDH was assayed as loading control. **e**, Efficiency of the combined treatment of Geldanamycin and Radicicol in disrupting the α-Synuclein/Hsp90 interaction. HEK-293 cells were treated with Geldanamycin and Radicicol for 4 or 24 hours and then electroporated with recombinant α-Synuclein using the protocol for in-cell NMR experiments. Whole cell lysates were collected and used in immunoprecipitation assays with anti-α-Synuclein antibodies. The obtained precipitates were then resolved in SDS-PAGE and analyzed by Western blot using the indicated antibodies. In addition to HEK-293 cells with normal levels of Hsp90 (control cells), cells with reduced levels of Hsp90 (shHsp90) were used to validate the Hsp90 band. **f,** Inhibition of both Hsp90 and Hsc70 promotes α-Synuclein aggregation. The image shows a representative semi-quantitative Western blot of Hsc70-depleted HEK-293 cells treated with Geldanamycin and Radicicol. After 24 hours of treatment the cells were subjected to electroporation with recombinant α-Synuclein and 4 hours post electroporation the cells were harvested and subjected to Western blot. HMW and 14 kDa refer to high-molecular weight and monomeric α-Synuclein-species, respectively. **g**, **h**, Quantification of intracellular levels of Hsp90 and electroporated α-Synuclein in HEK-293 cells by Parallel Reaction Monitoring mass spectrometry (PRM). A standard curve (contained in the yellow boxes) using increasing amounts of recombinant Hsp90 (**g**) or α-Synuclein (**h**) serves for relative quantification of the intracellular protein levels. As surrogates for intracellular protein levels, at least four tryptic peptides of Hsp90 (**g**) or human α-Synuclein (**h**) were quantified. Targeted peptides are shown in the top of each plot, and at least four transitions of the y-series of the product ions were monitored over the chromatographic separation of the peptides (different colors). The determined cellular concentrations of Hsp90 and α-Synuclein were 30 μM and 2.5 μM, respectively (see Supplementary Methods section for details of this calculation). cps; counts per second. The original and uncropped gels of panels **a** as well as **c–f** can be found in Supplementary Figure 1. Western Blot and PCR experiments (panels **a, c–f**) were done in duplicates resulting in similar results.

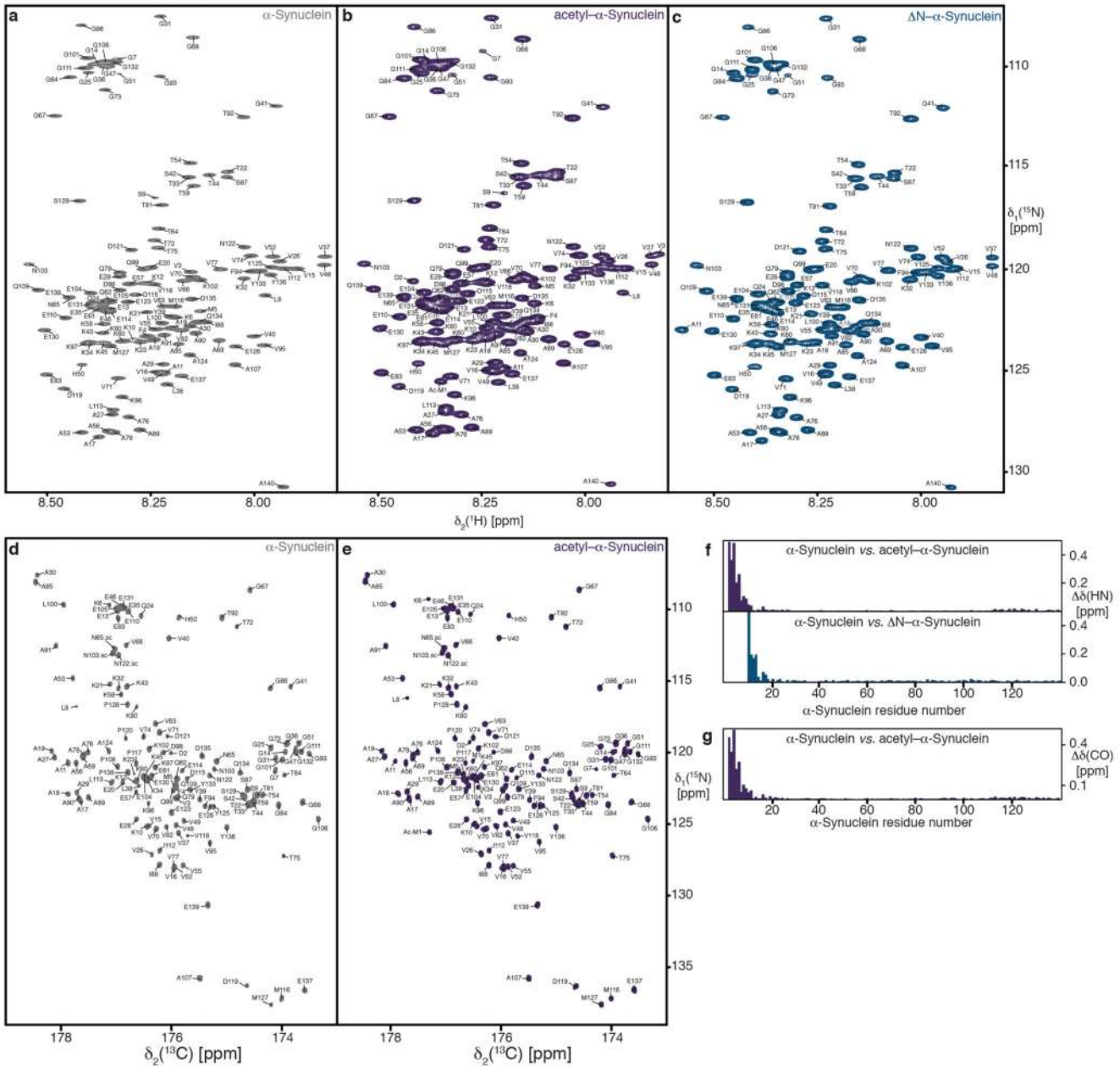

Extended Data Figure 8. Sequence-specific NMR-resonance assignments of α-Synuclein variants.

a–c, 2D [^{15}N,^{1}H]-NMR spectra of 500 μM [*U*-^{13}C,^{15}N]–α-Synuclein (grey), 450 μM [*U*-^{13}C,^{15}N]–acetyl–α-Synuclein (dark-violet), and 100 μM [*U*-^{15}N]–ΔN–α-Synuclein (dark blue). The sequence-specific resonance assignments for wild-type as well as acetylated–α-Synuclein obtained from 3D triple resonance experiments and from chemical shift mapping for ΔN–α-Synuclein are indicated. **d, e,** 2D [^{13}C,^{15}N]-NMR spectra of 500 μM [*U*-^{13}C,^{15}N]–α-Synuclein (grey) and 450 μM [*U*-^{13}C,^{15}N]–acetyl–α-Synuclein (dark-violet). The sequence-specific resonance assignments for wild-type and acetylated–α-Synuclein obtained from 3D triple resonance experiments are indicated. **f,** Residue-resolved combined chemical-shift perturbations of the amide moieties for acetyl–α-Synuclein (dark violet) and ΔN–α-

Synuclein (dark blue) *vs.* wild-type α-Synuclein. **g,** Residue-resolved combined chemical-shift difference of the carbonyl-amide moieties for acetyl–α-Synuclein (dark violet) *vs.* wild-type α-Synuclein. [^{15}N,^{1}H]-NMR spectra in panels **a–c** were measured several times (n=5), and [^{13}C,^{15}N]-NMR spectra (panels **d, e**) were measured in duplicates, all yielding similar results.

Europe PMC Funders Author Manuscripts

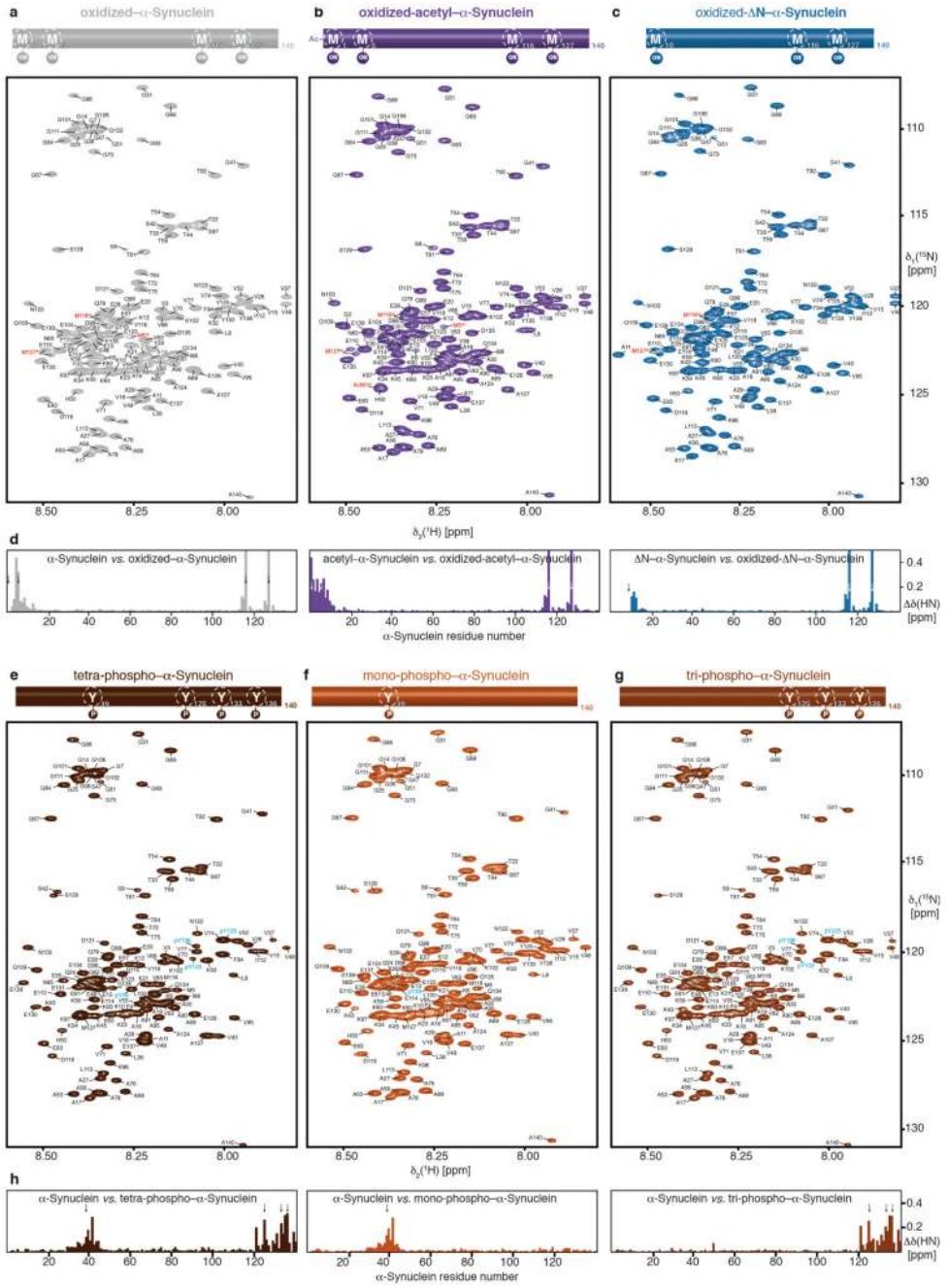

Extended Data Figure 9. Sequence-specific NMR-resonance assignments of methionine-oxidized and tyrosine-phosphorylated α-Synuclein variants.

a–c, 2D [^{15}N,^{1}H]-NMR spectra of 100 μM [*U*-^{15}N]–oxidized–α-Synuclein (light grey), 100 μM [*U*-^{15}N]–oxidized-acetyl–α-Synuclein (violet), and 100 μM [*U*-^{15}N]–oxidized-ΔN–α-Synuclein (blue). The sequence-specific resonance assignments from chemical shift mapping and published assignments of the oxidized state [23] are indicated. Oxidized methionines are highlighted in red. **d,** Residue-resolved combined chemical-shift differences of the amide moieties for oxidized–α-Synuclein (light grey), oxidized-acetyl–α-Synuclein

(violet), and oxidized-ΔN–α-Synuclein (blue) relative to their respective reduced states. Colors as in panels **a–c**. Arrows indicate the positions of the oxidized methionines. **e–g,** 2D [^{15}N,^{1}H]-NMR spectra of 50 μM [*U*-^{15}N]–mono-phospho–α-Synuclein (red-brown), 50 μM [*U*-^{15}N]–tri-phospho–α-Synuclein (brown), and 50 μM [*U*-^{15}N]–tetra-phospho–α-Synuclein (dark brown). The sequence-specific resonance assignments based on published assignments for phosphorylated α-Synuclein are indicated [24]. Phosphorylated residues are highlighted in cyan. **h,** Residue-resolved combined chemical-shift differences of the amide moieties for the phosphorylated–α-Synuclein variants relative to wild-type α-Synuclein. Colors as in panels **e–g**. Arrows indicate the positions of the phosphorylated tyrosines. [^{15}N,^{1}H]-NMR spectra of the different modified α-Synuclein variants were measured several times (n=4) yielding similar results.

Europe PMC Funders Author Manuscripts

Europe PMC Funders Author Manuscripts

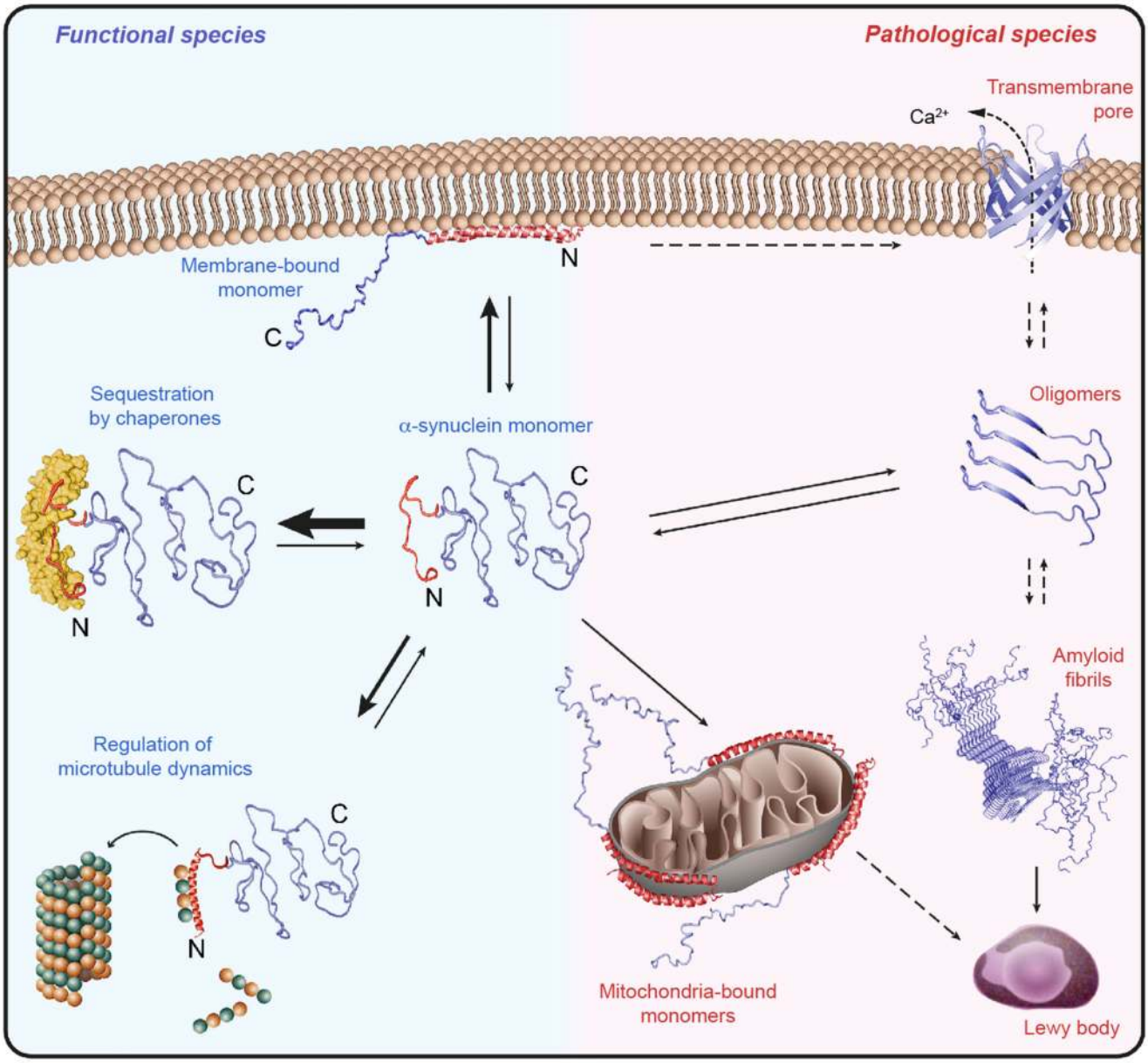

Extended Data Figure 10. Mechanism of chaperone-controlled regulation of α-Synuclein function, conformation, and localization, in mammalian cells.

Cellular chaperones (yellow) interact with the amino-terminal segment of α-Synuclein (red), thus actively regulating its functional species by shifting conformational equilibria. Impairing the natural α-Synuclein–chaperone ratio or deteriorations of the α-Synuclein–chaperone interaction by post-translational modifications can consequently favor the formation of pathological species, including the association of α-Synuclein to mitochondria.

Supplementary Material

Refer to Web version on PubMed Central for supplementary material.

Acknowledgements

We thank S. Grzesiek (Basel), D. Otzen (Aarhus), M. Goedert (Cambridge), B. Bukau (Heidelberg), D.P. Mulvihill (Kent), and D. Kahne (Harvard) for providing plasmids. Further, we thank T. Maier (Basel) and M. Plodinec (Basel) for providing mammalian cell lines, E. Stuttfeld and D. Asgeirsson for technical help with cell culture experiments, and V. Juvin (SciArtWork) for help with graphic design. The Swedish NMR Centre of the University of Gothenburg is acknowledged for spectrometer time. This work was supported by the Swiss National Science Foundation (PP00P3_128419 to S.H., Ambizione Fellowship PZ00P3_148238 to B.M.B., and Marie Heim-Vögtlin PMPDP3_164425 to S.C.) as well as the European Research Council (FP7 contract MOMP 281764 to S.H.). B.M.B. also gratefully acknowledges funding from the Swedish Research Council and the Knut och Alice Wallenberg Foundation through a Wallenberg Academy Fellowship as well as through the Wallenberg Centre for Molecular and Translational Medicine, University of Gothenburg, Sweden.

References

1. Goedert M, Spillantini MG, Del Tredici K, Braak H. 100 years of Lewy pathology. Nat Rev Neurol. 2013; 9:13–24. [PubMed: 23183883]
2. Barnham KJ, Masters CL, Bush AI. Neurodegenerative diseases and oxidative stress. Nat Rev Drug Discov. 2004; 3:205–214. [PubMed: 15031734]
3. Lashuel HA, Overk CR, Oueslati A, Masliah E. The many faces of α-Synuclein: from structure and toxicity to therapeutic target. Nat Rev Neurosci. 2013; 14:38–48. [PubMed: 23254192]
4. Hantschel O, Superti-Furga G. Regulation of the c-Abl and Bcr-Abl tyrosine kinases. Nat Rev Mol Cell Biol. 2004; 5:33–44. [PubMed: 14708008]
5. Mahul-Mellier AL, et al. c-Abl phosphorylates α-Synuclein and regulates its degradation: implication for α-Synuclein clearance and contribution to the pathogenesis of Parkinson's disease. Hum Mol Genet. 2014; 23:2858–2879. [PubMed: 24412932]
6. Dedmon MM, Christodoulou J, Wilson MR, Dobson CM. Heat shock protein 70 inhibits α-Synuclein fibril formation *via* preferential binding to prefibrillar species. J Biol Chem. 2005; 280:14733–14740. [PubMed: 15671022]
7. Dimant H, Ebrahimi-Fakhari D, McLean PJ. Molecular chaperones and co-chaperones in Parkinson disease. Neuroscientist. 2012; 18:589–601. [PubMed: 22829394]
8. Pemberton S, et al. Hsc70 protein interaction with soluble and fibrillar α-Synuclein. J Biol Chem. 2011; 286:34690–34699. [PubMed: 21832061]
9. Theillet FX, et al. Structural disorder of monomeric α-Synuclein persists in mammalian cells. Nature. 2016; 530:45–50. [PubMed: 26808899]
10. Burmann BM, Wang C, Hiller S. Conformation and dynamics of the periplasmic membrane-protein–chaperone complexes OmpX-Skp and tOmpA-Skp. Nat Struct Mol Biol. 2013; 20:1265–1272. [PubMed: 24077225]
11. He L, Sharpe T, Mazur A, Hiller S. A molecular mechanism of chaperone-client recognition. Sci Adv. 2016; 2:e1601625. [PubMed: 28138538]
12. Falsone SF, Kungl AJ, Rek A, Cappai R, Zangger K. The molecular chaperone Hsp90 modulates intermediate steps of amyloid assembly of the Parkinson-related protein α-Synuclein. J Biol Chem. 2009; 284:31190–31199. [PubMed: 19759002]
13. Karagöz GE, et al. Hsp90-Tau complex reveals molecular basis for specificity in chaperone action. Cell. 2014; 156:963–974. [PubMed: 24581495]
14. Schopf FH, Biebl MM, Buchner J. The HSP90 chaperone machinery. Nat Rev Mol Cell Biol. 2017; 18:345–360. [PubMed: 28429788]
15. Roodveldt C, et al. Chaperone proteostasis in Parkinson's disease: stabilization of the Hsp70/α-Synuclein complex by Hip. EMBO J. 2009; 28:3758–3770. [PubMed: 19875982]
16. Gao X, et al. Human Hsp70 disaggregase reverses Parkinson's-linked α-Synuclein amyloid fibrils. Mol Cell. 2015; 59:781–793. [PubMed: 26300264]
17. Finn TE, Nunez AC, Sunde M, Easterbrook-Smith SB. Serum albumin prevents protein aggregation and amyloid formation and retains chaperone-like activity in the presence of physiological ligands. J Biol Chem. 2012; 287:21530–21540. [PubMed: 22549788]

18. Wilhelm BG, et al. Composition of isolated synaptic boutons reveals the amounts of vesicle trafficking proteins. Science. 2014; 344:1023–1028. [PubMed: 24876496]
19. Maltsev AS, Ying J, Bax A. Impact of N-terminal acetylation of α-Synuclein on its random coil and lipid binding properties. Biochemistry. 2012; 51:5004–5013. [PubMed: 22694188]
20. Kim YE, Hipp MS, Bracher A, Hayer-Hartl M, Hartl FU. Molecular chaperone functions in protein folding and proteostasis. Annu Rev Biochem. 2013; 82:323–355. [PubMed: 23746257]
21. McNulty BC, Young GB, Pielak GJ. Macromolecular crowding in the *Escherichia coli* periplasm maintains α-Synuclein disorder. J Mol Biol. 2006; 355:893–897. [PubMed: 16343531]
22. Cremades N, et al. Direct observation of the interconversion of normal and toxic forms of α-synuclein. Cell. 2012; 149:1048–1059. [PubMed: 22632969]
23. Binolfi A, et al. Intracellular repair of oxidation-damaged α-Synuclein fails to target C-terminal modification sites. Nat Commun. 2016; 7
24. Kosten J, et al. Efficient modification of α-Synuclein serine 129 by protein kinase CK1 requires phosphorylation of tyrosine 125 as a priming event. ACS Chem Neurosci. 2014; 5:1203–1208. [PubMed: 25320964]
25. Brahmachari S, et al. Activation of tyrosine kinase c-Abl contributes to α-Synuclein-induced neurodegeneration. J Clin Invest. 2016; 126:2970–2988. [PubMed: 27348587]
26. Shahmoradian SH, et al. Lewy pathology in Parkinson's disease consists of crowded organelles and lipid membranes. Nat Neurosci. 2019; 22:1099–1109. [PubMed: 31235907]
27. Mahul-Mellier AL, et al. The making of a Lewy body: the role of α-synuclein post-fibrillization modifications in regulating the formation and the maturation of pathological inclusions. bioRxiv. 2018
28. Fusco G, et al. Structural basis of membrane disruption and cellular toxicity by α-Synuclein oligomers. Science. 2017; 358:1440–1443. [PubMed: 29242346]
29. Guardia-Laguarta C, Area-Gomez E, Schon EA, Przedborski S. Novel subcellular localization for α-synuclein: possible functional consequences. Front Neuroanat. 2015; 9:17. [PubMed: 25755636]
30. Park JS, Davis RL, Sue CM. Mitochondrial dysfunction in Parkinson's Disease: new mechanistic insights and therapeutic perspectives. Curr Neurol Neurosci Rep. 2018; 18:21. [PubMed: 29616350]
31. Reeve AK, et al. Mitochondrial dysfunction within the synapses of *substantia nigra* neurons in Parkinson's disease. NPJ Parkinsons Dis. 2018; 4:9. [PubMed: 29872690]
32. Korndörfer IP, Dommel MK, Skerra A. Structure of the periplasmic chaperone Skp suggests functional similarity with cytosolic chaperones despite differing architecture. Nat Struct Mol Biol. 2004; 11:1015–1020. [PubMed: 15361861]
33. Ferbitz L, et al. Trigger factor in complex with the ribosome forms a molecular cradle for nascent proteins. Nature. 2004; 431:590–596. [PubMed: 15334087]
34. Saio T, Guan X, Rossi P, Economou A, Kalodimos CG. Structural basis for protein antiaggregation activity of the Trigger Factor chaperone. Science. 2014; 344
35. Bull HB, Breese K. Surface tension of amino acid solutions: a hydrophobicity scale of the amino acid residues. Arch Biochem Biophys. 1974; 161:665–670. [PubMed: 4839053]
36. Rüdiger S, Germeroth L, Schneider-Mergener J, Bukau B. Substrate specificity of the DnaK chaperone determined by screening cellulose-bound peptide libraries. EMBO J. 1997; 16:1501–1507. [PubMed: 9130695]
37. Banerjee PR, Moosa MM, Deniz AA. Two-dimensional crowding uncovers a hidden conformation of α-Synuclein. Angew Chem Int Ed Engl. 2016; 55:12789–12792. [PubMed: 27612332]

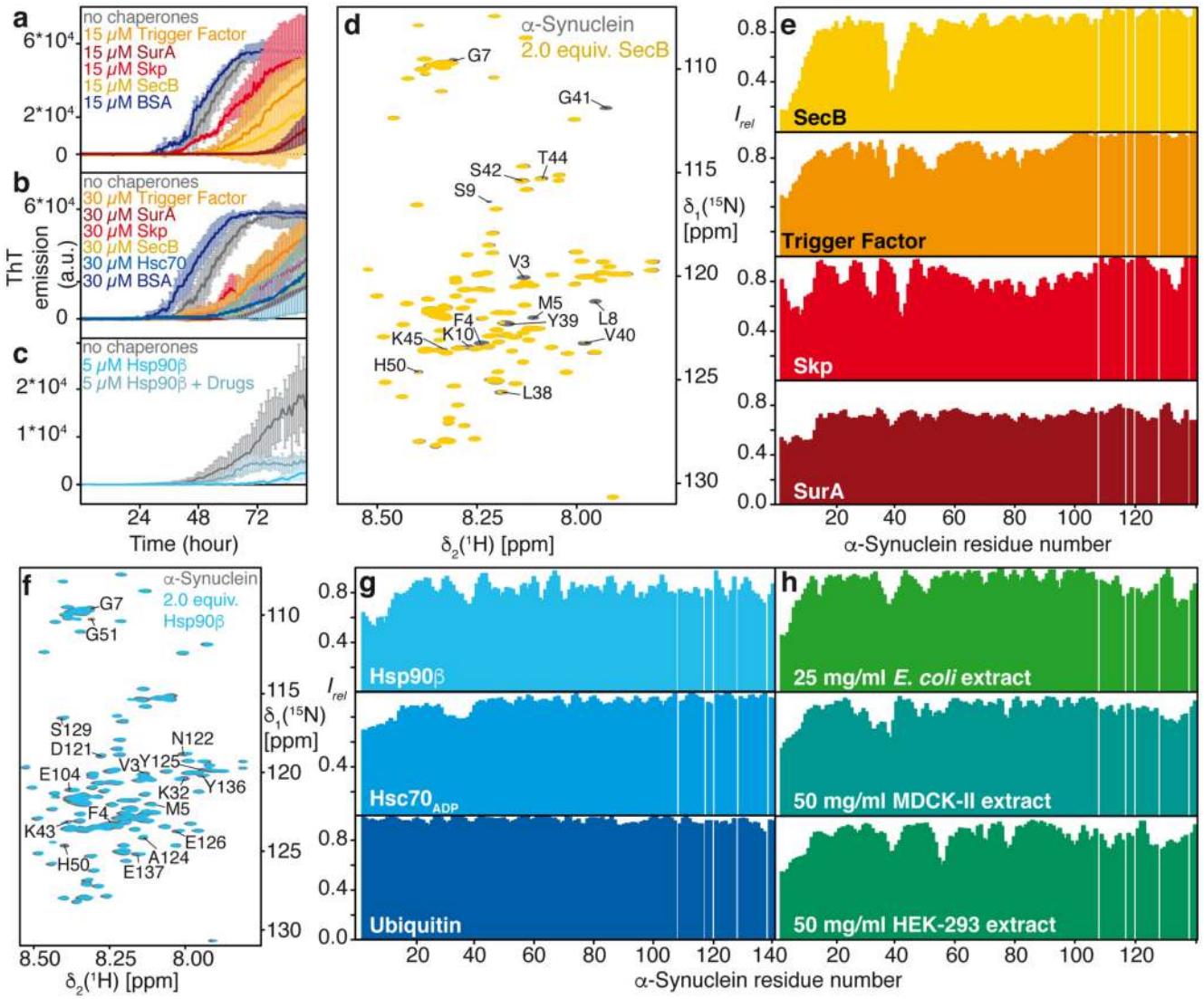

Figure 1. Molecular chaperones delay α-Synuclein aggregation by interaction with its amino-terminus.

a, b, ThT emission curves of 300 μM α-Synuclein in the presence of chaperones (15 μM in (**a**) and 30 μM in (**b**)). **c,** ThT emission curves of 100 μM α-Synuclein in the presence of 5 μM Hsp90β with and without addition of 1 μM of Drugs. In panels **a-c**, mean values are given with SD (n=3). **d,** Overlay of 2D [^{15}N, ^{1}H]-NMR spectra of 250 μM [*U*-^{15}N]–α-Synuclein in the absence (grey) and presence of 500 μM of SecB-tetramer (yellow) (n=3, with similar results). **e,** Residue-resolved backbone amide NMR signal attenuation (I_{rel} = I/I_0) of α-Synuclein upon addition of two equivalents of either SecB tetramer (yellow), Trigger Factor dimer (orange), Skp trimer (red), and SurA dimer (dark red). **f,** Overlay of 2D [^{15}N,^{1}H]-NMR spectra of [*U*-^{15}N]–α-Synuclein in the absence (grey) and presence of two equivalents Hsp90β-dimer (cyan) (n=2, with similar results). **g, h,** Residue-resolved backbone amide NMR signal attenuation (I_{rel} = I/I_0) of α-Synuclein upon addition of two equivalents of Hsp90β-dimer (cyan), $Hsc70_{ADP}$ (light-blue), and Ubiquitin (dark blue) as

Europe PMC Funders Author Manuscripts

well as *E. coli* cell-extract (green), mammalian MDCK-II cell-extract (blue), and mammalian HEK-293 cell-extract (green). In panels **e**, **g**, and **h**, values < 1.0 are indicative of intermolecular interactions.

Europe PMC Funders Author Manuscripts

Europe PMC Funders Author Manuscripts

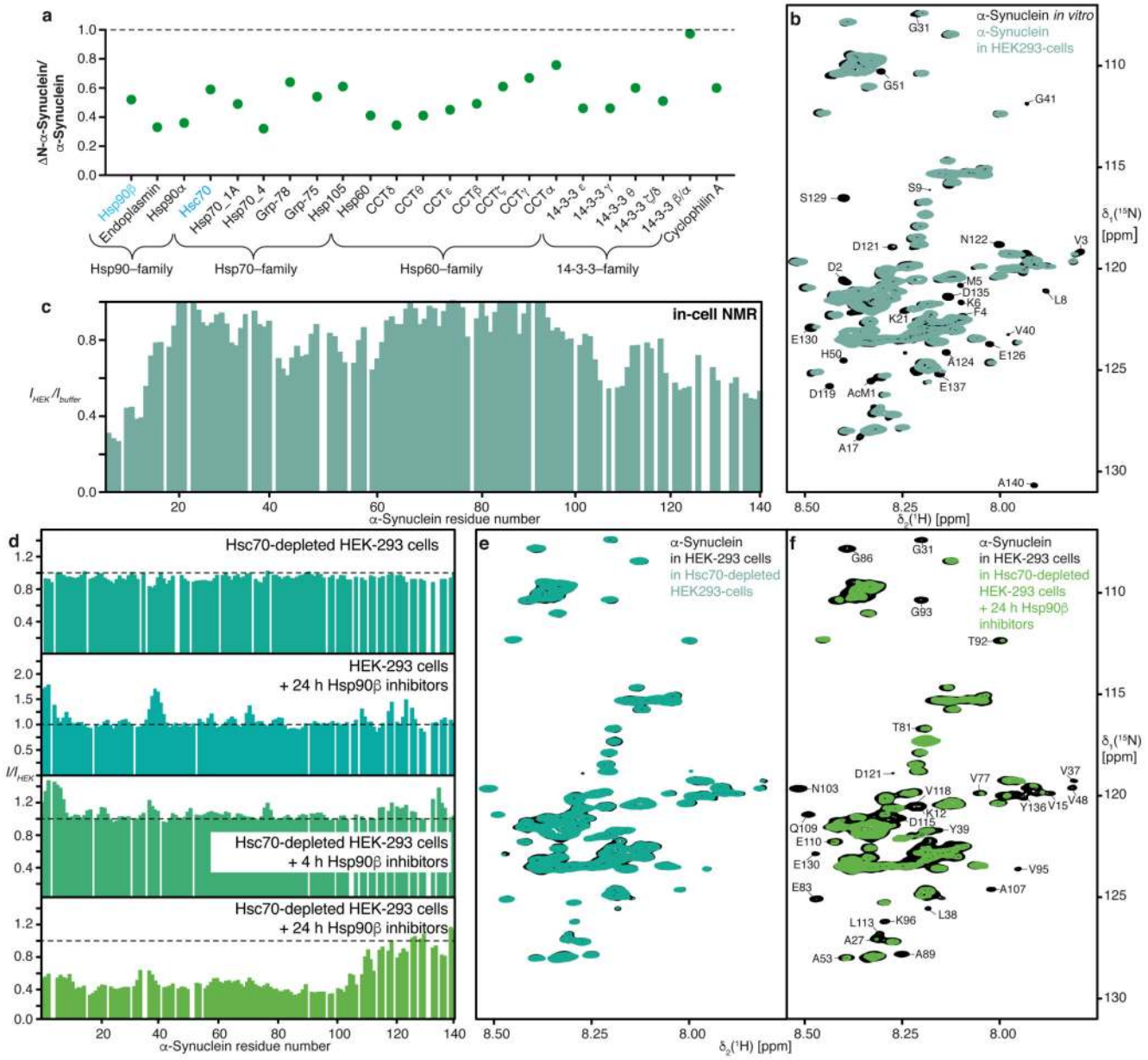

Figure 2. The interaction between α-Synuclein and chaperones is dominant in living cells.

a, Abundance ratios of proteins bound to ΔN–α-Synuclein *vs.* wild-type full-length α-Synuclein determined by relative quantitative mass-spectrometry (mean values, n=2). **b,** Overlay of 2D [^{15}N,^{1}H]-NMR spectra of [*U*-^{15}N]–α-Synuclein in NMR-buffer (black) and inside living HEK-293 cells (blue-green). Representative spectrum from n>5. **c,** Residue-resolved backbone amide NMR signal attenuation ($I_{HEK}/I_{\mathrm{Buffer}}$) of α-Synuclein in mammalian cells. **d,** In-cell NMR signal attenuation in differently treated cells, relative to untreated cells (I/I_{HEK}). Different combinations of Hsc70-depletion and Hsp90β-inhibition were applied, as indicated. **e, f,** Overlay of 2D [^{15}N,^{1}H]-NMR spectra of [*U*-^{15}N]–α-Synuclein in untreated HEK-293 cells (black) and in Hsc70-depleted HEK-293 cells (green)

(**e**) or in Hsc70-depleted HEK-293 cells after 24 hours of Hsp90β-inhibition (green) (**f**). Representative data (**d–f**) for three technical replicates yielding similar results.

Europe PMC Funders Author Manuscripts

Europe PMC Funders Author Manuscripts

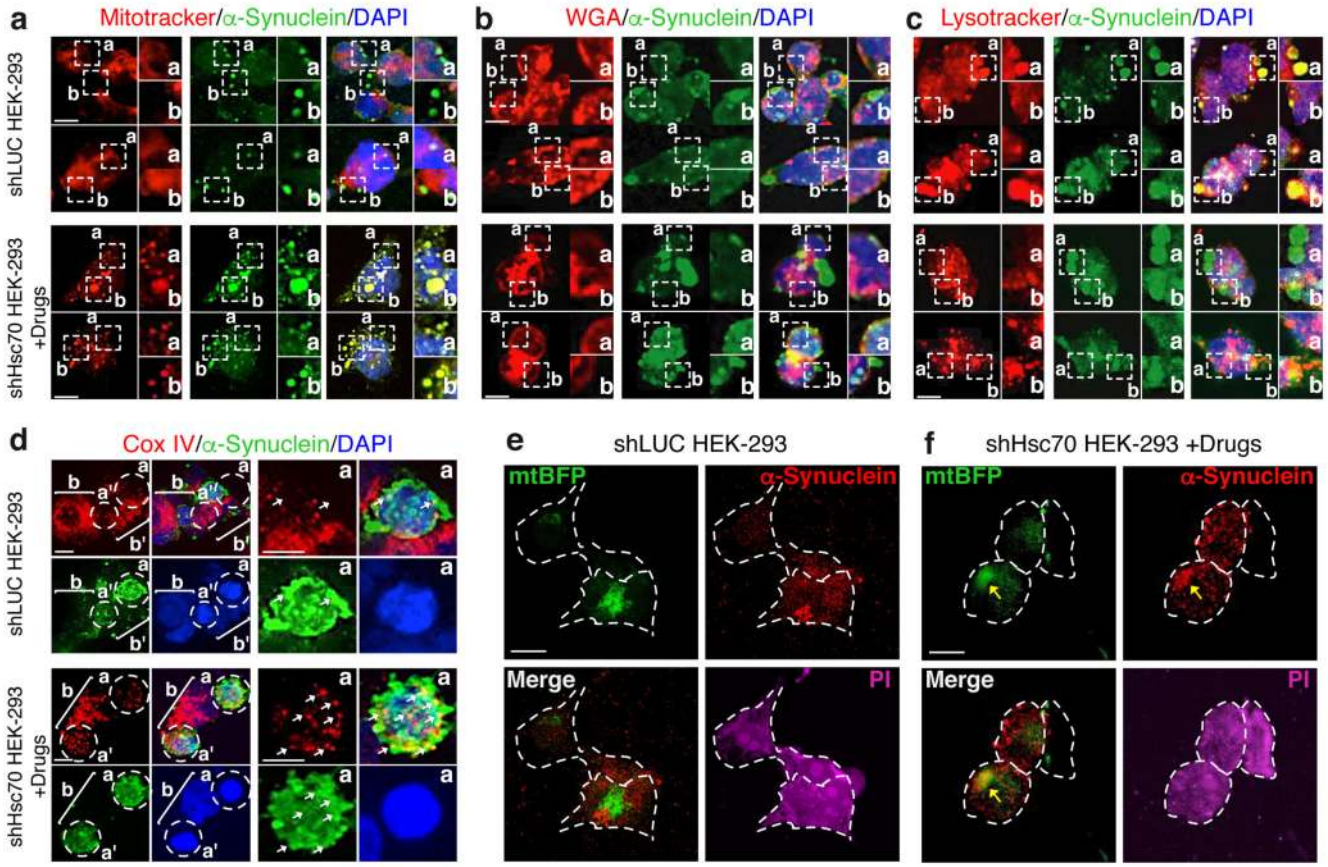

Figure 3. Co-localization of α-Synuclein and cellular organelles by immunofluorescence.

a–f, Immunofluorescence analysis of α-Synuclein electroporated into HEK-293 cells. Cells were either untreated (shLuc) or treated for a combined depletion of Hsc70 and Hsp90β (shHsc70 + Drugs). Cells were either stained with mitotracker (red; **a**) to stain mitochondria, or with WGA (red; **b**) to stain the plasma membrane and the endoplasmatic reticulum or lysotracker (red, **c**) to stain acidic vesicles such as lysosomes, DAPI (blue) to stain cell nuclei, and an α-Synuclein specific antibody (green). Dashed boxes indicate areas of intense signal for mitotracker and α-Synuclein. **d,** Cox IV (red, mitochondrial marker) and α-Synuclein (green) were visualized by specific antibodies, nuclei were stained by DAPI (blue). Dashed circles labeled a or a' indicate cells with high α-Synuclein content, brackets labeled b or b' indicate cells with low α-Synuclein content. **e, f**, Control HEK-293 cells (shLuc; **e**) or HEK-293 cells treated for the combined knock-down of Hsc70 and Hsp90β (shHsc70 + Drugs; **f**) were stably transfected with an expression plasmid containing the gene of mitochondria-targeted blue fluorescent protein (mtBFP). Cells were fixed and subjected to immunofluorescence analyses using an anti-α-Synuclein antibody. Propidium iodide (PI) was used to stain cells un-specifically allowing visualization of cell morphology. Note, the blue color originating from mtBFP was changed to green to better visualize mtBFP/α-Synuclein co-localization. Scale bar in all panels: 10 μm. Experiments were performed twice yielding similar results.

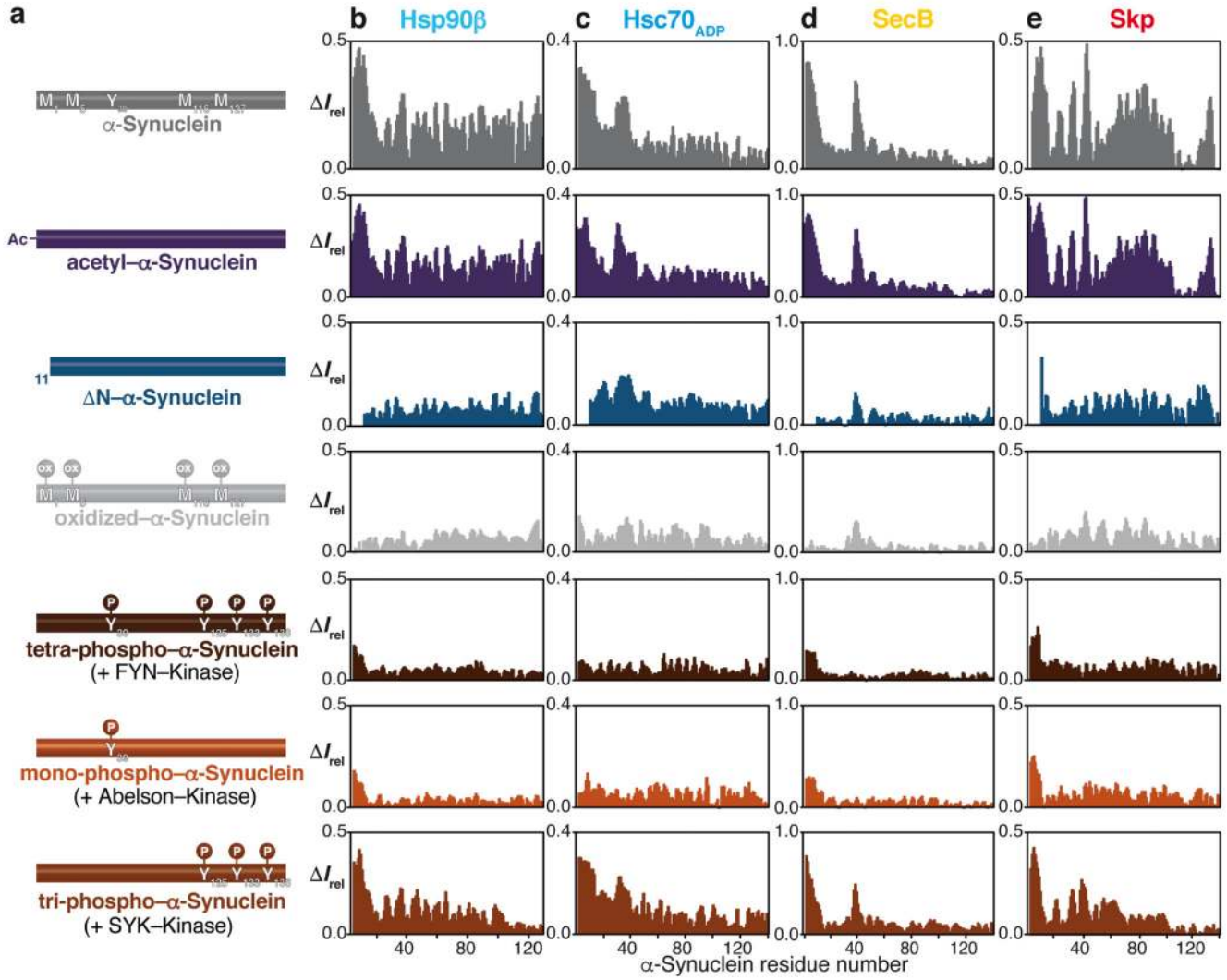

Figure 4. Effect of post-translational modifications on the chaperone–α-Synuclein interaction.

a, Cartoon representation of differently modified α-Synuclein variants as indicated. **b, c, d, and e**, Residue-resolved backbone amide NMR signal attenuation ($\Delta I_{rel} = 1 - I/I_0$) of the α-Synuclein variants upon interaction with two equivalents of Hsp90β dimer (**b**), $Hsc70_{ADP}$ (**c**), SecB tetramer (**d**) or Skp trimer (**e**). Elevated ΔI_{rel} values are indicative of an interaction.

Europe PMC Funders Author Manuscripts